Synergistic effects of ivabradine and metformin in the treatment of concomitant chronic heart failure and diabetes mellitus by regulating the activity of the H19/miR-423-5p/HCN4 axis

Fang Zhang[1], Weijun Jiang[1], Yating Liu[1], Liu Li[1], Rui Wang[2], Yang Li[3]

[1]Department II of Ultrasound Diagnosis, The First Hospital of Qinhuangdao
[2]Department I of Endocrinology, The First Hospital of Qinhuangdao
[3]Department of Research, The First Hospital of Qinhuangdao

Corresponding author:
Fang Zhang
Department II of Ultrasound Diagnosis
The First Hospital of Qinhuangdao
No. 258 Wenhua Road
Haigang District,
Qinhuangdao 066000, Hebei Province, China
E-mail: heartsung@yeah.net

Submitted: 28 May 2019; **Accepted:** 1 November 2019
Online publication: 26 March 2021

Arch Med Sci
DOI: https://doi.org/10.5114/aoms/113625

Abstract

Introduction: As a type of frequently diagnosed heart disease, chronic heart failure (CHF) is characterized by high mortality and morbidity. Previous studies have shown that ivabradine (IBD) could exert a therapeutic effect in CHF patients, and that the presence of diabetes mellitus (DM) may reduce the therapeutic effect of IBD in the treatment of CHF. Moreover, metformin (MET) was shown to induce the methylation of H19, which may enable MET to function as a sensitizer of IBD in the treatment of CHF, especially in those with DM. Therefore, in this study, we investigated the molecular mechanisms underlying the therapeutic effect of MET and IBD in the treatment of CHF and DM.

Material and methods: SD rat model groups were established as a CHF + streptozotocin (STZ) + MET group, a CHF + IBD group, a CHF + STZ + IBD group, and a CH + STZ + IBD + MET group, with 20 rats in each group. Basic and cardiac indexes were measured to study the therapeutic effects of MET and IBD via transthoracic echocardiography. Real-time PCR, ELISA, immunohistochemistry (IHC) assays and Western blot assay were conducted to observe the expression of H19, miR-423-5p, NE, BNP-45 and HCN4. In silico analysis and luciferase assays were further conducted to establish the signaling pathway and clarify the molecular mechanisms underlying the interaction between MET and IBD.

Results: MET administration restored the normal values of general/cardiac indexes in CHF rats. The abnormal values of echocardiographic indexes in CHF rats with STZ-induced DM were all corrected to a certain degree after MET administration. Moreover, the injection of STZ up-regulated the expression of plasma NE/BNP-45, while IBD administration reduced the levels of NE/BNP-45 in CHF rats. Furthermore, the administration of MET reduced the NE level in CHF rats, indicating that both MET and IBD can exert a therapeutic effect on CHF rats. Additionally, in silico analysis and luciferase assays verified the role of H19 and HCN4 as target genes of miR-423-5p. In fact, the transfection of MET or H19 siRNA1/2 into HL-1 and H9C2 cells down-regulated the levels of H19 and HCN4 while increasing the level of miR-423-5p.

Conclusions: MET reduces H19 expression via inducing methylation of its promoter, and the inhibited H19 expression suppresses HCN4 expression by up-regulating miR-423-5p expression. As a result, the suppressed expression of HCN4 reduces the heart rate and exhibits a therapeutic effect in the treatment of concomitant CHF and DM.

Key words: chronic heart failure, diabetes mellitus, ivabradine, metformin, H19, miR-423-5p, HCN4.

Introduction

As a type of frequently diagnosed heart disease, chronic heart failure (CHF) is characterized by high mortality and morbidity rates [1]. Currently, about 2% of adults in Western countries suffer from CHF, while the prevalence of CHF rises above 10% in patients older than 70 years [2]. Although significant progress has been made in the treatment of CHF along with a decreased period of hospitalization required for many CHF patients, a European Society of Cardiology Heart Failure (ESC-HF) pilot study conducted in Europe showed that the 12-month mortality among hospitalized CHF patients was still as high as about 20% [3]. In addition, the prevalence of CHF increases with age and the presence of chronic diseases, including type 2 diabetes mellitus (T2DM), obesity, and hypertension [4]. Moreover, due to the current epidemic of obesity and diabetes, the incidence of CHF has been gradually increasing in recent years [5].

Hyperpolarization-activated cyclic nucleotide-gated (HCN) ion channels, coded by HCN 1–4 genes, are responsible for the generation of hyperpolarization-activated current. Containing four isotypes, the HCN family can modulate synaptic integration and intrinsic neuronal excitability [6, 7]. In addition, the presence of cyclic adenosine monophosphate (cAMP) can induce activation of HCN channels [8]. Therefore, the activation of HCN channels is increased by cAMP-coupled receptors. In particular, among the four members of the HCN family, HCN4 shows the highest affinity for cAMP [9]. Moreover, gene microarrays have implicated the upregulation of HCN4 expression in the impairment of human ventricular functions [10]. For example, it was suggested that the upregulation of HCN4 expression in the atrial tissues contributes to the elevated level of atrial ectopic beat upon atrial dilation. Therefore, potential inhibitors of HCN channels, including ivabradine (IBD) and zatebradine, may be used in the clinical treatment of CHF-induced atrial tachyarrhythmias [11].

As a specific inhibitor of HCN channels located in cardiac pacemaker cells [12], IBD can lead to a reduced heart rate during both exercise and resting states, without exerting any effect on blood pressure or cardiac contractility [13]. In fact, IBD was shown to exert a therapeutic effect in CHF patients by affecting the remodeling of the left ventricle [14, 15]. Moreover, it was revealed that IBD enhances cardiac functions by restoring the uptake-1 of norepinephrine (NE) via specific signaling pathways, thus decreasing the elevated levels of BNP-45 and NE in CHF [16]. Other findings suggested that the activity of IBD is inhibited in diabetic hyperglycemia, potentially caused by the impaired uptake-1 of NE [16].

Multiple classes of non-coding RNAs, such as long non-coding RNAs (lncRNAs) and microRNAs (miRNAs), have been shown to play essential roles in the regulation of gene expression [17]. Furthermore, lncRNAs can also regulate mRNA expression by inducing its translation or degradation [17]. For example, the hypermethylation of H19 promoter was found to reduce the level of H19 in both mouse and human [18, 19]. Moreover, it was shown that metformin (MET), a compound with both anti-cancer and anti-diabetic properties, reduces the expression of H19 by inducing the methylation of H19 [20].

Previous findings showed that the presence of diabetes mellitus (DM) may reduce the therapeutic effect of IBD in the treatment of CHF [16]. Meanwhile, it has also been shown that MET may reduce the expression of H19 by enhancing the methylation status of H19 promoter, which subsequently promotes the expression of miR-423-5p and suppresses the expression of HCN4, a target of miR-423-5p [17]. Therefore, we hypothesized that MET may function as a sensitizer of IBD in the treatment of CHF, especially in those with DM.

Therefore, with respect to the fact that MET could reduce the expression of H19 and H19 could influence the expression of miR-423-5p, we assumed that MET could reduce the expression of HCN4 via modulating the H19/miR-423-5p/HCN4 signaling in DM. Moreover, as the effect of IBD was suppressed by DM in the treatment of CHF, we focused the study on the possible synergistic effects of IBD and MET in the treatment of concomitant CHF and DM.

Material and methods

Animals and treatment

A total of 180 healthy male Sprague Dawley (SD) rats with an average body weight of about 200 g were purchased from the animal center of our institute and used in this study. All rats were kept in an SPF grade animal facility with a 12-h light/dark cycle, under a specific temperature (18–22°C), relative humidity (40–70%), and a noise level of < 50 dB, and were given ad libitum access to water and food. The rats were randomly assigned to 9 groups, i.e., a control group (sham-operated healthy SD rats), a streptozotocin (STZ) group, a STZ + MET group, a CHF group, a CHF + STZ group, a CHF + STZ + MET group, a CHF + IBD group, a CHF + STZ + IBD group, and a CHF + STZ + IBD + MET group, with 20 rats in each group. During the experiment, the rats in the groups involving MET treatment were given 250 mg/kg of MET via oral administration from day 1 to day 18 of the experiment. In the control group, the rats were given water to replace MET. The rats in the groups involving IBD treatment were given 10 mg/kg of IBD (Sigma-Aldrich, St. Louis, MO) via daily i.p. injection after the establishment of

the CHF model was completed. The rats in other groups were treated according to the procedures described below. The experimental protocol and animal use plan in this study were approved by the Animal Ethics Committee of our institute, while all experiments were carried out in strict accordance with National Institutes of Health (NIH) guidelines.

Induction of diabetes

STZ (Sigma-Aldrich, St. Louis, MO) was dissolved in saline and given to rats in a single dose of 70 mg/kg via i.p. injection to induce diabetes. The presence of diabetes was confirmed 4 weeks later by the measurement of blood glucose level. A blood glucose level of > 350 mg/dl was considered as the criterion for the successful modeling of diabetic rats.

Establishment of chronic heart failure

The CHF rats were generated via coronary artery ligation. In brief, the rats were anesthetized through inhalation of a mixture of oxygen with 5% isoflurane. Subsequently, the rats underwent left thoracotomy performed between the 4th and the 5th ribs. After the left ventricular wall was carefully exposed, myocardial infarction was induced by permanently ligating the left anterior descending artery using a polypropylene suture. In the next step, the lungs of the rats were hyper-inflated via positive end-expiratory pressure. Subsequently, the chest opening in the rats was sutured and the survival of rats was monitored for 24 h.

Size of myocardial infarction and left ventricular function

At about 7 weeks after establishing the model, the rats were anesthetized to measure their dimensions of the left ventricle and heart rate using transthoracic echocardiography. A phased array transducer was used to carry out the measurements according to the manufacturer's instructions. In addition, at the end of each measurement, a catheter was placed in the right carotid artery of the rats to determine the arterial blood pressure and the left ventricular end-diastolic pressure, the two parameters later used to evaluate the cardiac functions of the rats in different groups. All rats were euthanized at the end of experiment and the heart of each rat was removed to estimate the size of the myocardial infarction according to the method described in the literature [28–31].

Measurements of norepinephrine and BNP-45 by ELISA

The expression of NE and BNP-45 in the rats of different groups was measured using aortic blood samples, while the uptake-1 of NE was measured using myocardium tissue samples taken from healthy tissues adjacent to the infarcted tissues of the stellate ganglion collected from each rat. In brief, after blood samples were collected from the aorta, they were immediately transferred into EDTA-coated blood sampling tubes. Subsequently, the levels of NE and BNP-45 in blood samples were measured using corresponding ELISA kits (RapidBio Systems, Minneapolis, MN) following the instructions of the manufacturer. During the measurement, the antigens were diluted at a ratio of 1 : 20, and 100 µl of standard diluent was added to each well of the ELISA plate and then incubated at 4°C overnight. On the next day, diluted samples and HRP-labeled substrate were added to the ELISA plate and incubated in the dark at 37°C for 20 min. When an obvious color change occurred in the positive control, or when a slight color change occurred in the negative control, the reaction in the wells was terminated by the addition of 50 µl of a terminating reagent. Within 20 min, the optical density (OD) value of each well was measured at a wavelength of 450 nm on a microplate reader (SpectraMax M5, Molecular Devices, San Jose, CA). The uptake of NE in stellate ganglion tissue samples was measured in a similar way after the tissue samples were homogenized into a homogenate by a blender.

RNA isolation and real-time PCR

Total RNA was extracted from tissue and cell samples using a TRIZOL kit (Invitrogen, Carlsbad, CA) in strict accordance with the kit instructions. RNA concentration was determined using a spectrometer. Primers for H19, miR-423-5p, and HCN4 mRNA were synthesized by Takara (Tokyo, Japan). Reverse transcription was performed using a reverse transcription kit (Thermo Fisher Scientific, Waltham, MA) with reference to the manufacturer's instructions. The reaction conditions of reverse transcription were as follows: 50 min of reverse transcription at 42oC followed by 5 s of reverse transcriptase inactivation at 85oC. The obtained cDNA was then diluted to 50 ng/µl for subsequent real-time PCR. The amplification system of qPCR contained 25 µl. The real-time PCR was performed on an ABI 7900 real-time PCR instrument (ABI, Foster City, CA). The real-time PCR conditions were as follows: pre-denaturation at 95oC for 4 min, followed by 30 cycles of denaturation at 95oC for 30 s, annealing at 57oC for 30 s and extension at 72oC for 30 s. A total of 2 µg of cDNA was used as the qPCR template for each target gene, while β-actin was used as the internal reference. The 2-ΔΔCt method was used to calculate the relative expression of H19, miR-423-5p, and HCN4 mRNA. The primer pairs

usedwere:H19-F:5'-TGCTGCACTTTACAACCACTG-3'; H19-R:5'-ATGGTGTCTTTGATGTTGGGC-3';miR-423-5p-F:5'-GGCTGAGGGGCAGAGAG-3';miR-423-5p-R: 5'-GTGCAGGGTCCGAGGT-3'; HCN4-F: 5'-CCCAAGA ACCTTCCCGAGTG-3'; HCN4-R: 5'-GATGTCTTCCGAG GCAGAGTGA-3'.

Cell culture and transfection

HL-1 and H9C2 cells were purchased from the Cell Bank of the Chinese Academy of Sciences and cultured at 37°C and 5% CO_2 in Dulbecco's Modified Eagle Medium (DMEM) (Gibco, Carlsbad, CA) containing 10% fetal bovine serum (Gibco, Carlsbad, CA), 100 µg/ml penicillin and 100 µg/ml streptomycin (Invitrogen, Carlsbad, CA). The cells were harvested during logarithmic growth by trypsinization and then sub-cultured 1–2 times a week. For MET treatment, the cells were incubated with 0.5 µM or 1 µM of MET for 48 h before the cells were harvested for analysis. In addition, to test the effect of H19 on the expression of miR-423-5p and HCN4, HL-1 and H9C2 cells were transfected with H19 siRNA1 or siRNA2 using Lipofectamine 2000 (Invitrogen, Carlsbad, CA) in accordance with the instructions provided by the manufacturer. The cells were harvested at 48 h after transfection and used for subsequent experiments.

Vector construction, mutagenesis and luciferase assay

To clarify the regulatory relationship between miR-423-5p and H19/HCN4 mRNA, an online bioinformatics tool was used to locate potential binding sites of miR-423-5p in H19 and the 3' UTR of HCN4 mRNA. Subsequently, the full length of H19 as well as the 3' UTR of HCN4 mRNA containing the binding site of miR-423-5p was amplified by PCR and cloned into a pcDNA3.1 vector (Promega, Madison, WI). In addition, site-directed mutagenesis was carried out in the miR-423-5p binding sites of H19 and the 3' UTR of HCN4 mRNA, and the mutant sequences of H19 and the 3' UTR of HCN4 mRNA were inserted into pcDNA3.1 vectors to create the mutant plasmids of H19 and HCN4 mRNA, respectively. In the next step, HL-1 and H9C2 cells were co-transfected with miR-423-5p and mutant/wild type of H19 or HCN4 mRNA. After 48 h of transfection, the cells were collected and the luciferase activity of transfected cells was measured using a Dual-luciferase reporter gene assay system (Promega, Madison, WI), in which both the firefly luciferase activity of target genes and the Renilla luciferase activity of the internal control were measured. The expression of H19 or HCN4 mRNA was then calculated in terms of its relative luciferase activity.

Western blot analysis

Total protein was extracted from tissue and cell samples, resolved by 10% SDS-PAGE, and transferred onto a polyvinylidene fluoride (PVDF) membrane. The membrane was blocked with 5% bovine serum albumin at room temperature for 1 h, incubated with anti-HCN4 primary antibodies (ab32675, Abcam, Cambridge, MA) at 4°C overnight, incubated with HRP-labeled IgG secondary antibodies (ab6721, Abcam, Cambridge, MA) at room temperature for 1 h, colorized by an ECL reagent, and analyzed by Image J software to calculate the protein expression of HCN4, which was normalized to the expression of β-actin.

Immunohistochemistry

The expression of HCN4 in tissue samples was measured using conventional immunohistochemistry assays. IHC results were processed with ImageJ software.

Statistical analysis

All statistical analyses were conducted using SPSS 18 software (SPSS Inc., Chicago, IL). In addition, the comparisons between two groups were carried out by *t* test, while the comparisons among multiple groups were carried out by one-way analysis of variance (ANOVA), followed by Scheffe's test as the post hoc test. Each experiment was biologically repeated in triplicate. All results were original and strictly verified for their correctness. The measurement data were expressed as mean ± standard deviation. A p-value of < 0.05 was considered statistically significant.

Results

General/cardiac measurements of experimental rats

Figure 1 illustrates the changes of general/cardiac characteristics as well as echocardiographic values in the rats from the STZ, STZ + MET, CHF, CHF + STZ, CHF + STZ + MET, CHF + IBD, CHF + STZ + IBD, and CHF + STZ + IBD + MET groups (20 rats/group) in comparison with the values in the control group.

The concentrations of blood glucose (Figure 1 A) did not differ significantly after the induction of CHF, while evident increases in blood glucose concentrations were observed in the STZ, CHF + STZ, and CHF + STZ + IBD groups. Therefore, the body weight (Figure 1 B) of the rats exposed to STZ was slightly decreased. Meanwhile, body indexes, including heart weight (Figure 1 C), the ratio of heart weight/body weight (Figure 1 D), and infarct size (Figure 1 E), were all increased in CHF rats regardless of STZ exposure. Interestingly, the administra-

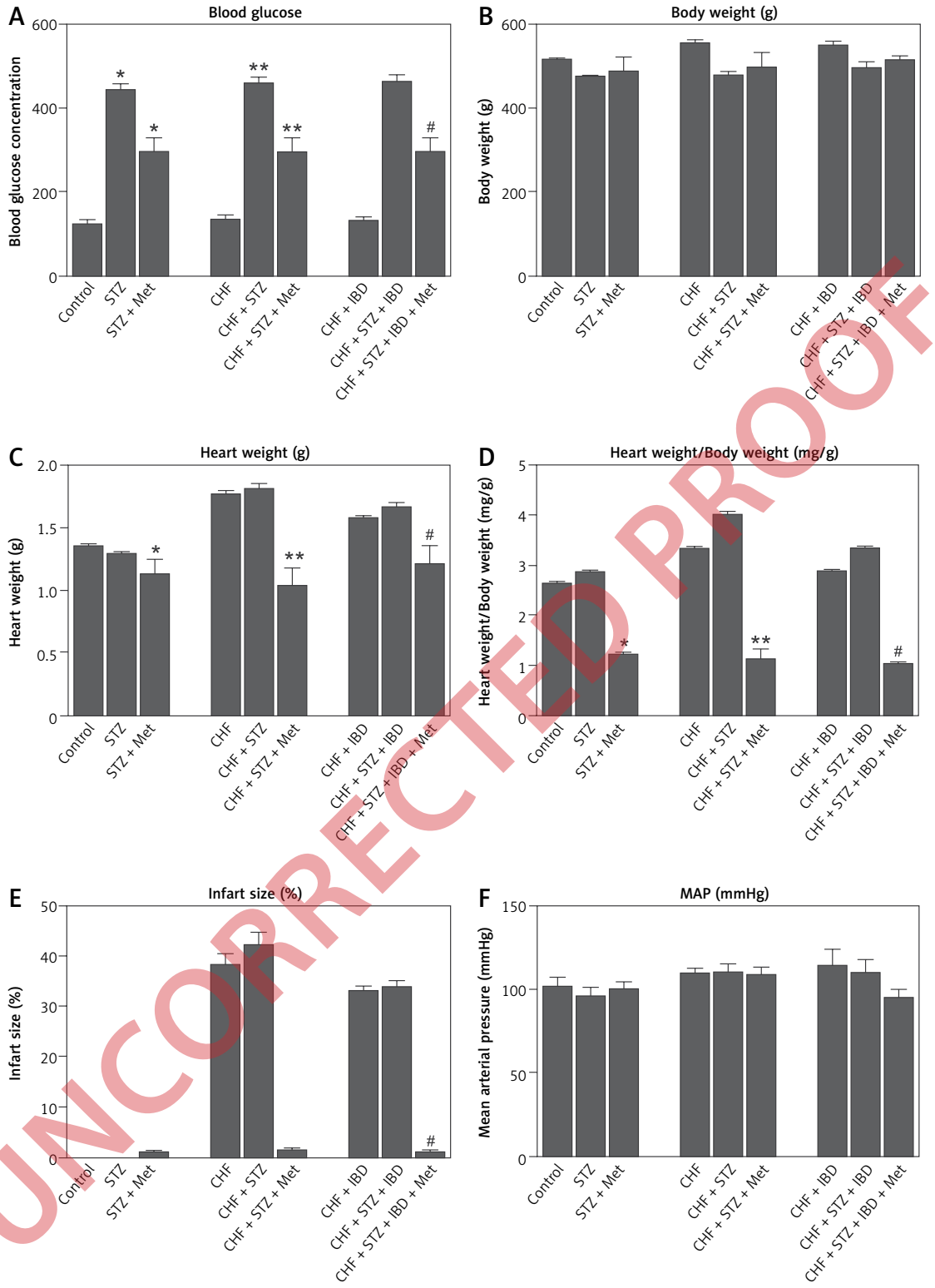

Figure 1. General/cardiac/echocardiographic measurements and the levels of NE/BNP-45 in the rats from the STZ, STZ + MET, CHF, CHF + STZ, CHF + STZ + MET, CHF + IBD, CHF + STZ + IBD, and CHF + STZ + IBD + MET groups (*p-value < 0.05, vs. control group; **p-value < 0.05, vs. CHF group; #p-value < 0.05, vs. CHF + STZ group). **A** – Concentration of blood glucose in rats from different groups. **B** – Body weight of rats from different groups. **C** – Heart weight of rats from different groups. **D** – Heart weight/body weight ratio of rats from different groups. **E** – Infarct size of rats from different groups. **F** – Mean arterial pressure (MAP) of rats from different groups.

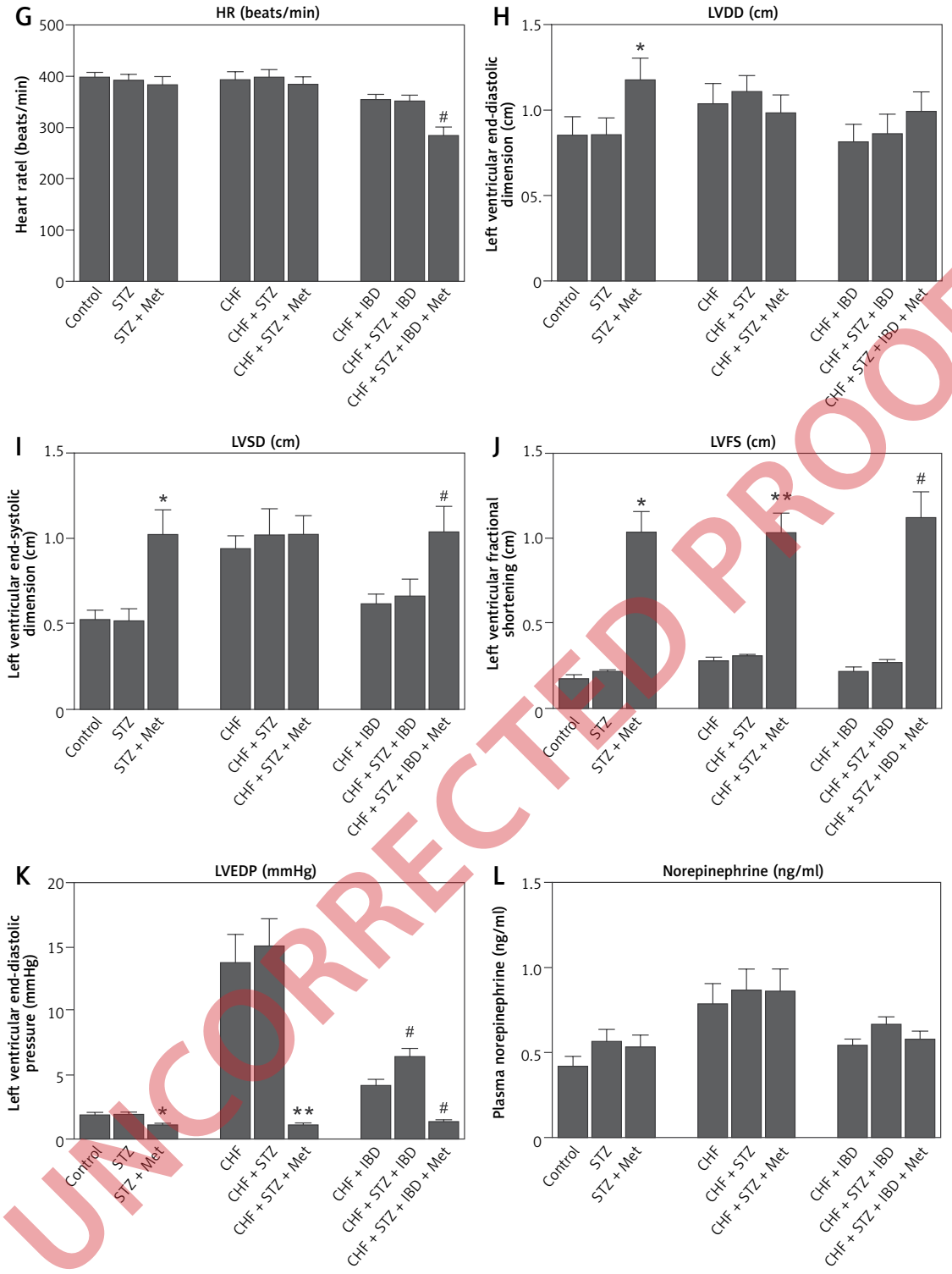

Figure 1. Cont. **G** – Heart rate (HR) of rats from different groups. **H** – LVDD of rats from different groups, **I** – LVSD of rats from different groups. **J** – LVFS of rats from different groups. **K** – LVEDP of rats from different groups. **L** – Level of plasma NE in rats from different groups. **M** – Level of BNP-45 in rats from different groups. **N** – SR of rats from different groups. **O** – CO of rats from different groups. **P** – CI of rats from different groups

tion of MET in STZ rats, CHF + STZ rats and CHF + STZ + IBD rats restored the general/cardiac characteristics of these rats to a level similar to that in the control rats, CHF rats and CHF + IBD rats. In addition, the value of mean arterial pressure (Figure 1 F) was not significantly altered among different groups, while a decreased heart rate (Figure 1 G) was only observed in CHF + IBD rats.

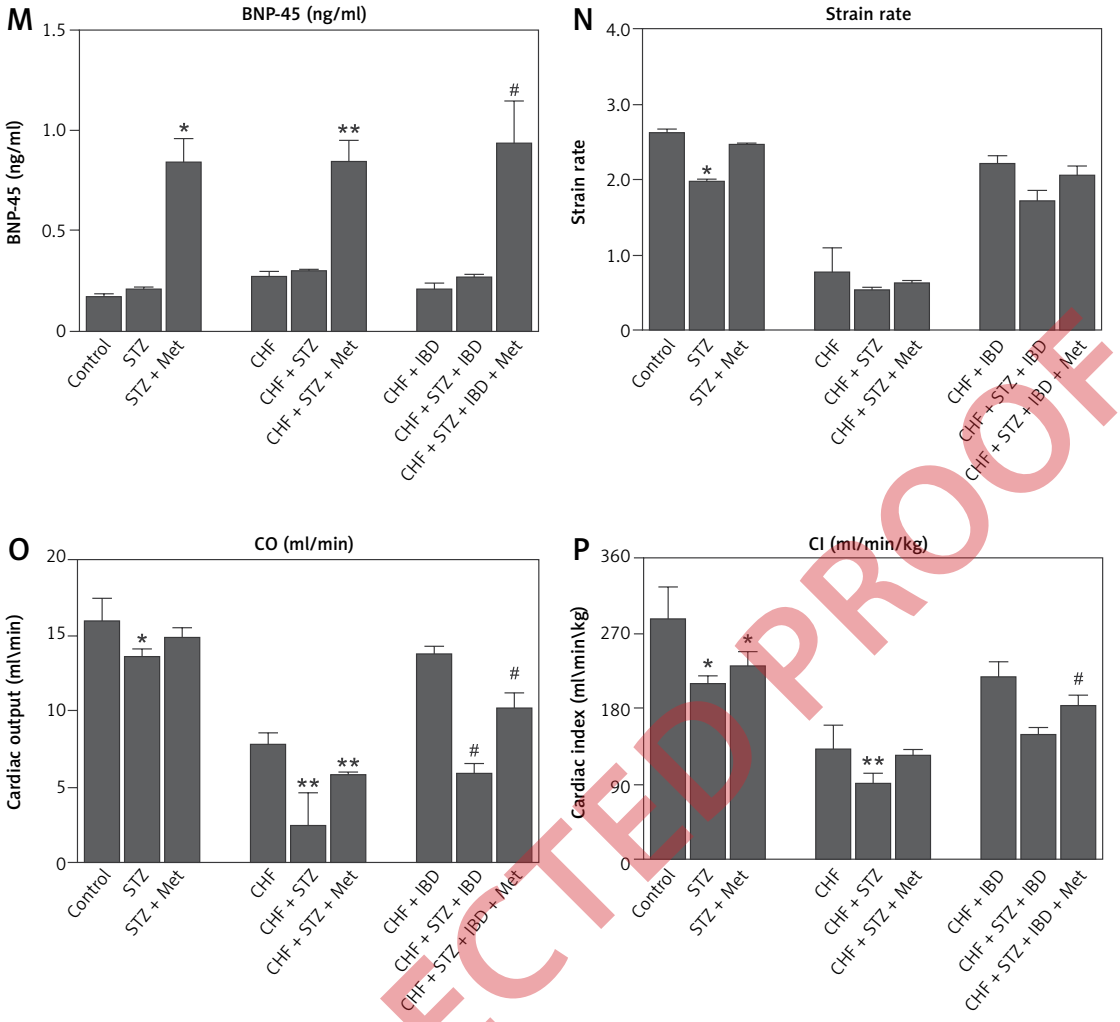

Figure 1. Cont. **M** – Level of BNP-45 in rats from different groups. **N** – SR of rats from different groups. **O** – CO of rats from different groups. **P** – CI of rats from different groups

Echocardiographic measurements in experimental rats

Subsequently, echocardiographic measurements were carried out to determine the values of left ventricular end-diastolic dimension (LVDD), left ventricular end-systolic dimension (LVSD), left ventricular fractional shortening (LVFS), left ventricular end- diastolic pressure (LVEDP), strain rate (SR), cardiac output (CO) and cardiac index (CI) in the rats from different groups. As the results show, the values of LVDD (Figure 1 H), LVSD (Figure 1 I) and LVEDP (Figure 1 K) were all increased in CHF rats compared with those in the control group, while the administration of IBD decreased the values of these indexes to a certain extent. In addition, all rats exposed to STZ showed higher index values compared with the rats not exposed to STZ. In contrast, the values of LVFS (Figure 1 J), SR (Figure 1 N), CO (Figure 1 O) and CI (Figure 1 P) were lower in CHF rats compared with those in the control group, while the administration of IBD evidently increased the corresponding values in CHF rats. Similarly, the rats exposed to STZ showed a lower value of LVFS, SR, CO and CI compared with the rats not exposed to STZ. Finally, the administration of MET in the rats exposed to STZ corrected the abnormal values of LVDD, LVSD, LVFS, LVEDP, SR, CO and CI to a certain extent.

Levels of NE and BNP-45 in experimental rats

As shown in Figure 1 L and compared with that in the control rats, the level of plasma NE was evidently elevated in CHF rats with or without STZ exposure, while the rats exposed to STZ showed a higher level of plasma NE than the rats not exposed to STZ. In addition, the CHF rats treated with IBD showed a lower level of NE than the CHF rats not treated with IBD, but a higher level of NE than control rats. Additionally, the administration of MET reduced the level of NE in the rats exposed to STZ. Similarly, the level of BNP-45 (Figure 1 M) showed a similar trend as that of NE. Therefore,

the changes in general/cardiac and echocardiographic indexes as well as the changes in NE and BNP-45 expression indicated that MET exerted a synergistic and therapeutic effect with IBD during CHF treatment.

Levels of H19, miR-423-5p and HCN4 in experimental rats

Levels of H19, miR-423-5p, and HCN4 in the rats from different groups were measured. An evident decrease in the expression of H19 (Figure 2 A) as well as in the mRNA (Figure 2 C) and protein (Figure 2 D) expression of HCN, along with a significantly increased level of miR-423-5p (Figure 2 B), was observed in the STZ + MET, CHF + STZ + MET, and CHF + STZ + IBD + MET groups. Moreover, when observing the methylation status of H19, MET was found to evidently promote H19 methylation compared with the other groups (Figure 2 E). In addition, IHC assays showed a reduced level of HCN protein (Figure 3) in the myocardial tissues collected from the rats in the STZ + MET, CHF + STZ + MET, and CHF + STZ + IBD + MET groups. Therefore, it can be assumed that the positive effects of MET on the activity of IBD during CHF treatment might be associated with the expression of H19, miR-423-5p and HCN4.

Association among H19, miR-423-5p and HCN4

Our in silico analyses revealed two conserved 'seed sequences' of miR-423-5p on H19 (Figure 4 A) and the 3'UTR of HCN4 (Figure 4 B). Subsequent luciferase assays showed that the luciferase activity of HL-1 cells co-transfected with miR-423-5p and wild-type H19 (Figure 4 A) or HCN4 (Figure 4 B) was apparently decreased, thus validating the role of H19 and HCN4 as target genes of miR-423-5p.

Molecular mechanism underlying the effect of MET in CHF treatment

The levels of H19 (Figure 4 C) and HCN4 mRNA (Figure 4 E)/protein (Figure 4 F) were evidently decreased, along with a significantly increased level of miR-423-5p (Figure 4 D), in HL-1 cells treated with 0.5 μM or 1 μM MET. Similarly, the transfection of HL-1 cells by H19 siRNA1 or H19 siRNA2 inhibited the expression of H19 (Figure 4 G) and HCN4 mRNA (Figure 4 I)/protein (Figure 4 J), along with highly up-regulated expression of miR-423-5p (Figure 4 H). In addition, similar results were obtained in H9C2 (Figure 5) cells treated with 0.5 μM/1 μM MET or H19 siRNA1/2.

In summary, the therapeutic effect of MET in CHF treatment and the synergistic effect of MET on IBD can be established by a potential molecular mechanism, in which MET exerts its inhibitory effect on H19 expression by enhancing the methylation of the H19 promoter. As a result, the inhibited H19 expression up-regulates the expression of miR-423-5p and reduces the expression of HCN4, which in turn reduces the heart rate and exhibits a therapeutic effect on CHF treatment.

Discussion

MET has been widely used in T2DM treatment since its approval in the U.S. and the U.K. in 1995 and 1958, respectively [21]. According to the guidelines published by the American Diabetes Association, MET is a first-line therapy used in the treatment of T2DM [22]. By reducing the intestinal absorption of glucose, MET can promote the uptake of peripheral glucose, enhance the sensitivity of the human body to insulin, and reduce the level of insulin in fasting plasma, thus resulting in a reduced level of blood glucose without causing hypoglycemia [23]. MET is also known to activate AMPK signaling and attenuate the severity of heart failure in dogs upon the induction of rapid ventricular pacing [24]. In addition, MET was found to reduce the degree of hypertrophy and fibrosis in mice subjected to chronic stress, while preserving the LV functions and promoting survival in mice following myocardial infarction [25, 26].

The exposure of human ovarian and endometrial cancer cells to MET can decrease the expression of H19, along with simultaneously increased methylation of the H19 promoter [27]. In addition, the inhibition of H19 expression by MET can activate SAHH and not only lead to DNA methylation but also induce the methylation of proteins involved in the regulation of chromatin structures [28]. In fact, the methylation of a specific gene is not only affected by the activation of DNA methyltransferases, but also by the alterations in proteins bound to chromatin [27]. In this study, an evident reduction in the expression of H19 and HCN was observed along with a significant increase in miR-423-5p expression after the administration of MET. In addition, similar results were observed in the myocardial tissues collected from experimental rats, thus validating the positive and synergistic effects of MET and IBD in the treatment of CHF, potentially by regulating the expression of H19, miR-423-5p and HCN4.

Recently, the involvement of the family of HCN channels in CHF has attracted great interest. HCN channels are associated with a depolarizing current known as the funny current (If), which is responsible for the activity of the cardiac pacemaker. So far, four genes, HCN1, HCN2, HCN3 and HCN4, have been identified as genes encoding HCN channels [29]. Among these four genes, the HCN4 gene is most highly expressed in the SA node of mam-

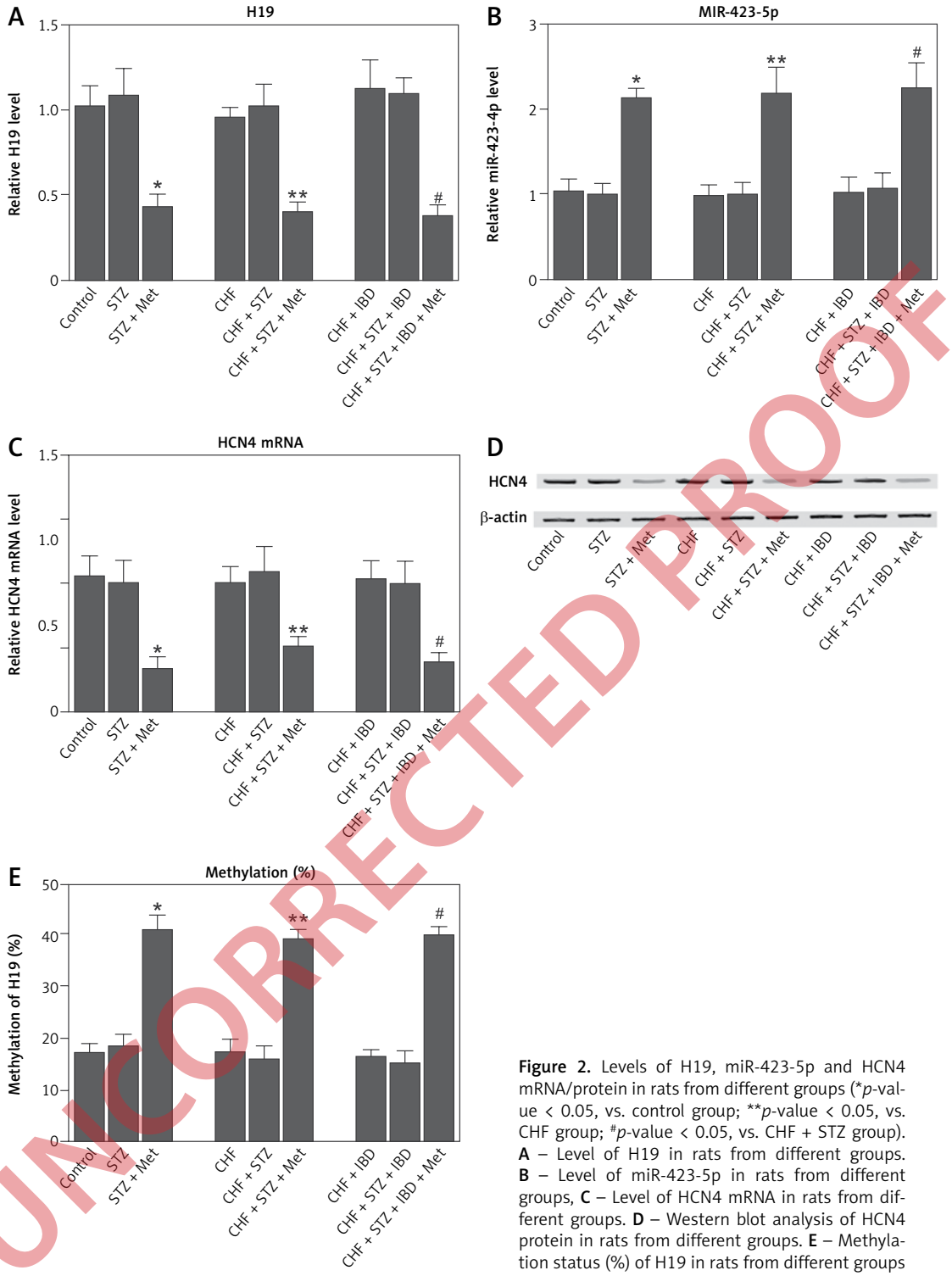

Figure 2. Levels of H19, miR-423-5p and HCN4 mRNA/protein in rats from different groups (**p*-value < 0.05, vs. control group; ***p*-value < 0.05, vs. CHF group; #*p*-value < 0.05, vs. CHF + STZ group). **A** – Level of H19 in rats from different groups. **B** – Level of miR-423-5p in rats from different groups, **C** – Level of HCN4 mRNA in rats from different groups. **D** – Western blot analysis of HCN4 protein in rats from different groups. **E** – Methylation status (%) of H19 in rats from different groups

malian adults [30]. For example, HCN4 accounts for nearly 80% of all HCN expression in humans [30]. Consistent with this observation, HCN4 mutations lacking the proper function of HCN4 have been implicated in inherited sinus bradycardia, thus suggesting the important role of HCN4 in the maintenance of a normal sinus rhythm [31]. While the global deletion of HCN4 in mice has been shown to induce embryonic lethality, other studies on HCN4-deficient embryos demonstrated an apparently decreased rate of cardiac contraction [32, 33]. It was also shown that as a target gene of miR-423-5p, the inhibition of HCN4 expression can lead to increased levels of both Nkx2.5 and miR-423-5p in the sinus node, which in turn cause bradycardia [34]. In this study, we observed that

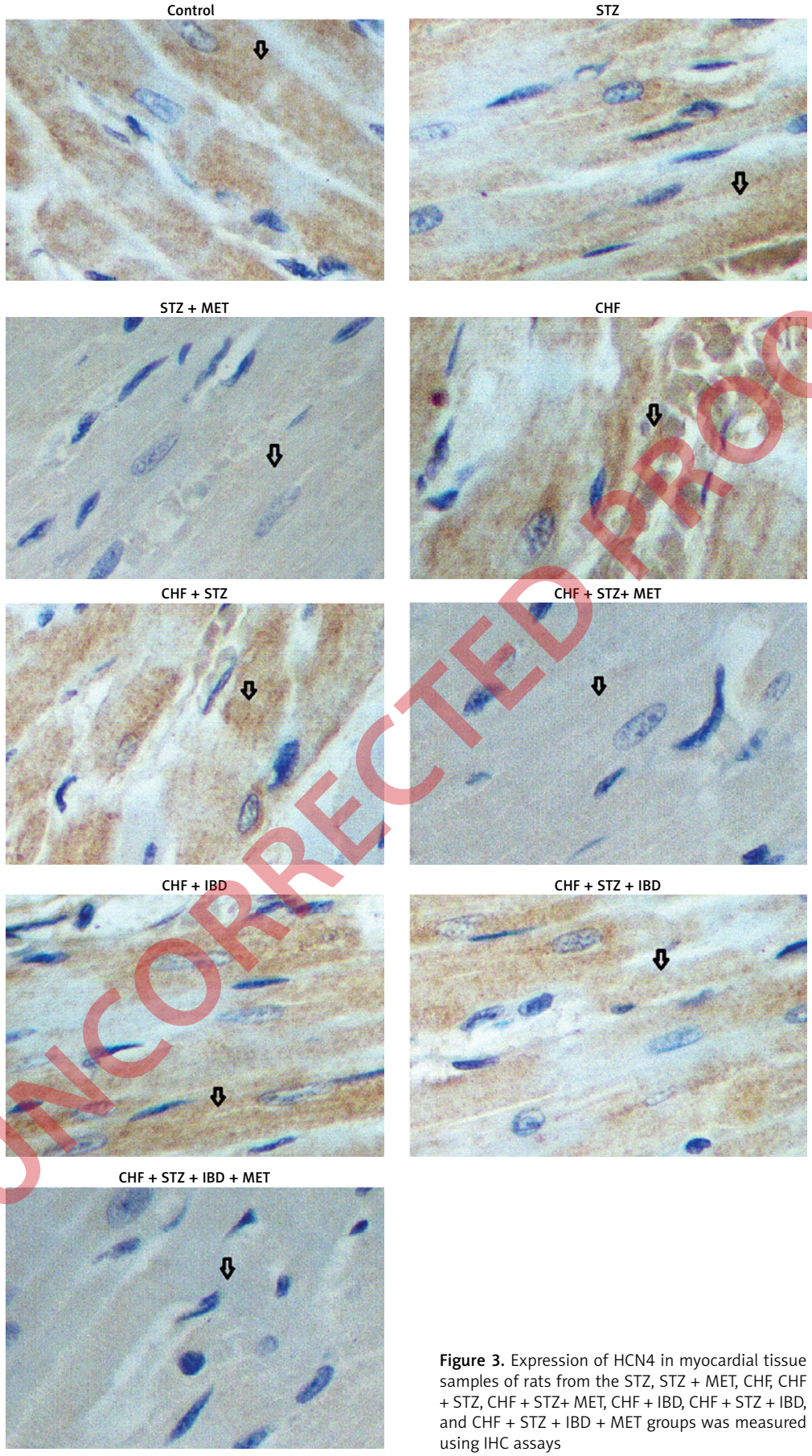

Figure 3. Expression of HCN4 in myocardial tissue samples of rats from the STZ, STZ + MET, CHF, CHF + STZ, CHF + STZ+ MET, CHF + IBD, CHF + STZ + IBD, and CHF + STZ + IBD + MET groups was measured using IHC assays

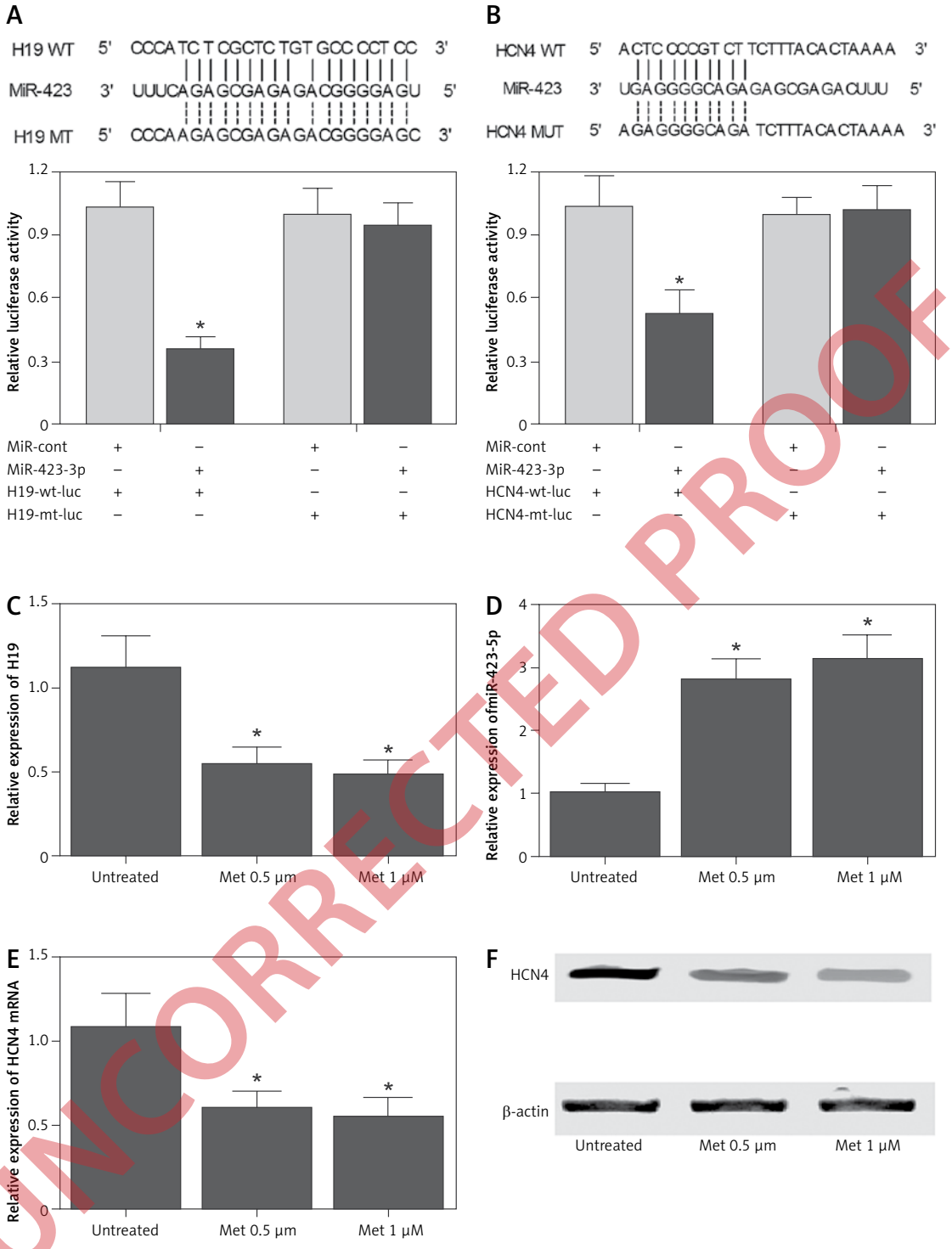

Figure 4. Associations among H19, miR-423-5p and HCN4 in HL-1 cells. **A** – In silico analysis for the relationship between miR-423-5p and H19, and luciferase assay of HL-1 cells co-transfected with wild-type/mutant H19 and miR-423-5p/control miRNA (*P value < 0.05, vs. miRNA controls). **B** – In silico analysis for the relationship between miR-423-5p and HCN4, and luciferase assay of HL-1 cells co-transfected with wild-type/mutant HCN4 and miR-423-5p/control miRNA (*P value < 0.05, vs. miRNA controls). **C** – Level of H19 in HL-1 cells treated with 0.5 μM or 1 μM MET compared with that in untreated HL-1 cells (*P value < 0.05, vs. untreated cells). **D** – Level of miR-423-5p in HL-1 cells treated with 0.5 μM or 1 μM MET compared with that in untreated HL-1 cells (* P value < 0.05, vs. untreated cells). **E** – Level of HCN4 mRNA in HL-1 cells treated with 0.5 μM or 1 μM MET compared with that in untreated HL-1 cells (*P value < 0.05, vs. untreated cells). **F** – Western blot analysis of HCN4 protein expressed in HL-1 cells treated with 0.5 μM or 1 μM MET compared with that in untreated HL-1 cells (* P value < 0.05, vs. untreated cells)

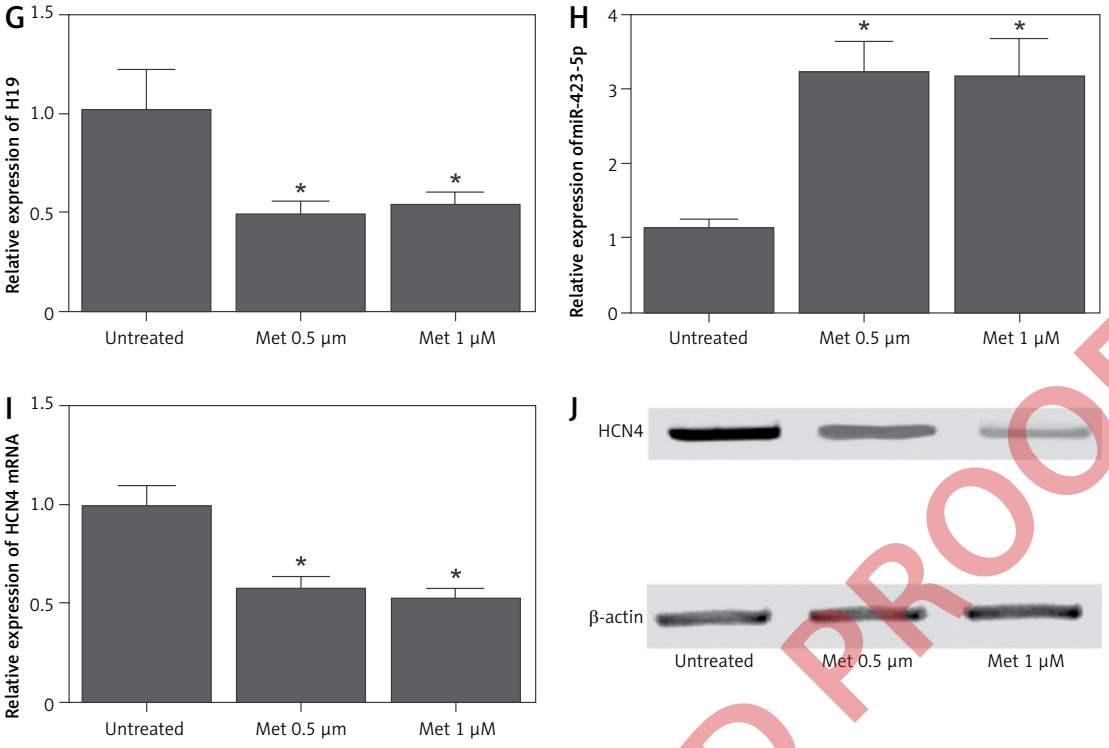

Figure 4. Cont. **G** – Level of H19 in HL-1 cells transfected with H19 siRNA 1 or H19 siRNA2 compared with that in HL-1 cells transfected with the negative control (*P value < 0.05, vs. untreated cells). **H** – Level of miR-423-5p in HL-1 cells transfected with H19 siRNA 1 or H19 siRNA2 compared with that in HL-1 cells transfected with the negative control (*P value < 0.05, vs. untreated cells). **I** – Level of HCN4 in HL-1 cells transfected with H19 siRNA 1 or H19 siRNA2 compared with that in HL-1 cells transfected with the negative control (*P value < 0.05, vs. untreated cells). **J** – Western blot analysis of HCN4 protein expression in HL-1 cells transfected with H19 siRNA 1 or H19 siRNA2 compared with that in HL-1 cells transfected with the negative control (* P value < 0.05, vs. untreated cells)

the levels of H19 and HCN4 were decreased along with an increased level of miR-423-5p after the transfection of MET or H19 siRNA1/2 into HL-1 and H9C2 cells.

The remodeling of HCN has been observed in both rodents and human athletes. In fact, miR-423-5p was shown to contribute to training-induced bradycardia by inhibiting the expression of HCN4 and affecting the heart rate [34]. Therefore, miR-423-5p may become a therapeutic target in the treatment of sinus node dysfunction in athletes [34]. As a pharmaceutical recently approved to treat chronic angina pectoris, IBD is especially helpful to treat patients who have a normal sinus rhythm but cannot be treated with beta blockers [35]. It was also shown that IBD can regulate If, a mixed Na^+-K^+ current induced by hyperpolarization and regulated by the autonomic nervous system [36]. Therefore, IBD can also be used to treat sinus tachycardia [37]. Moreover, IBD was found to play a protective role in the management of myocardial ischemic injury [38]. In fact, the beneficial value of IBD has been recognized in the treatment of chronic heart failure and in the prevention of cardiovascular death [38]. In particular, IBD was shown to reduce the heart rate in a mouse model of sinus tachycardia by upregulating the expression of HCN [39]. In contrast, it was found that the long-term administration of IBD in infarcted rats could partially alleviate the severity of cardiac remodeling by reducing the levels of HCN4 and HCN2 expression in atrial and ventricular cardiomyocytes [40]. Moreover, coronary artery diseases and diabetes are often concomitant, while prior studies showed that the mortality in myocardial infarction patients with diabetes is higher than that in myocardial infarction patients with no diabetes [41, 42]. In addition, the prevalence of heart failure in myocardial infarction patients with diabetes is also higher in spite of optimal treatment and prompt angioplasty [43]. Interestingly, a wide range of molecular and cellular processes have been implicated in the dysregulation of cardiac functions in myocardial infarction patients with diabetes [44]. For example, it was shown that IBD can significantly restore impaired uptake-1 of NE in the sympathetic ganglion and subsequently normalize the plasma level of NE in CHF rats [45]. Similarly, the effect of IBD on enhancing the uptake-1 of NE is impaired in STZ animals [16].

In conclusion, we observed for the first time that MET can improve the therapeutic effect of IBD in the treatment of concomitant CHF and DM via the H19/miR-423-5p/HCN4 axis. In fact,

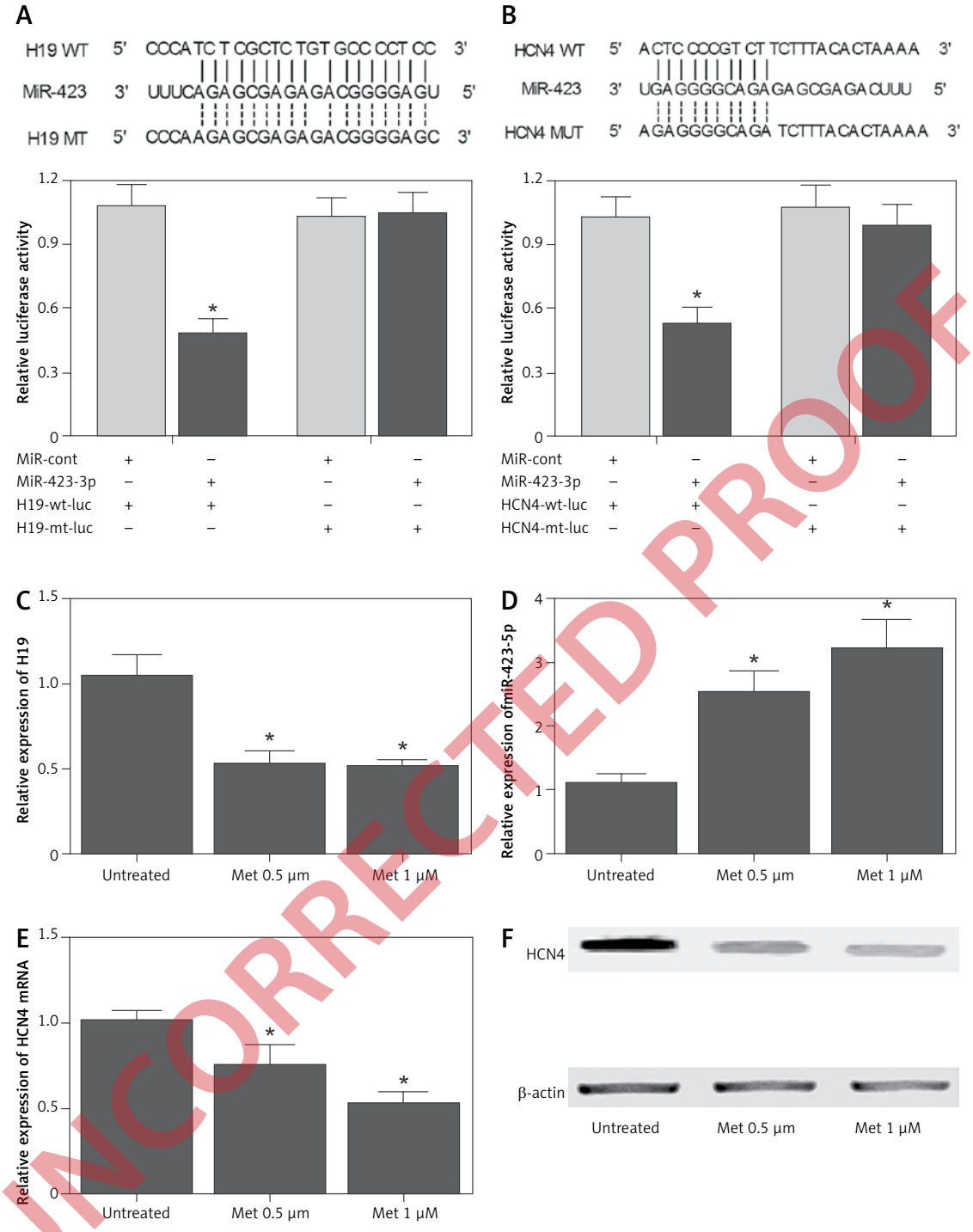

Figure 5. Associations among H19, miR-423-5p and HCN4 in H9C2 cells. **A** – In silico analysis for the relationship between miR-423-5p and H19, and luciferase assay of H9C2 cells co-transfected with wild-type/mutant H19 and miR-423-5p/control miRNA (**p*-value < 0.05, vs. miRNA controls). **B** – In silico analysis for the relationship between miR-423-5p and HCN4, and luciferase assay of H9C2 cells co-transfected with wild-type/mutant HCN4 and miR-423-5p/control miRNA (**p*-value < 0.05, vs. miRNA controls). **C** – Level of H19 in H9C2 cells treated with 0.5 μM or 1 μM MET compared with that in untreated H9C2 cells (**p*-value < 0.05, vs. untreated cells). **D** – Level of miR-423-5p in H9C2 cells treated with 0.5 μM or 1 μM MET compared with that in untreated H9C2 cells (**p*-value < 0.05, vs. untreated cells). **E** – Level of HCN4 mRNA in H9C2 cells treated with 0.5 μM or 1 μM MET compared with that in untreated H9C2 cells (**p*-value < 0.05, vs. untreated cells). **F** – Western blot analysis of HCN4 protein expressed in H9C2 cells treated with 0.5 μM or 1 μM MET compared with that in untreated H9C2 cells (**p*-value < 0.05, vs. untreated cells)

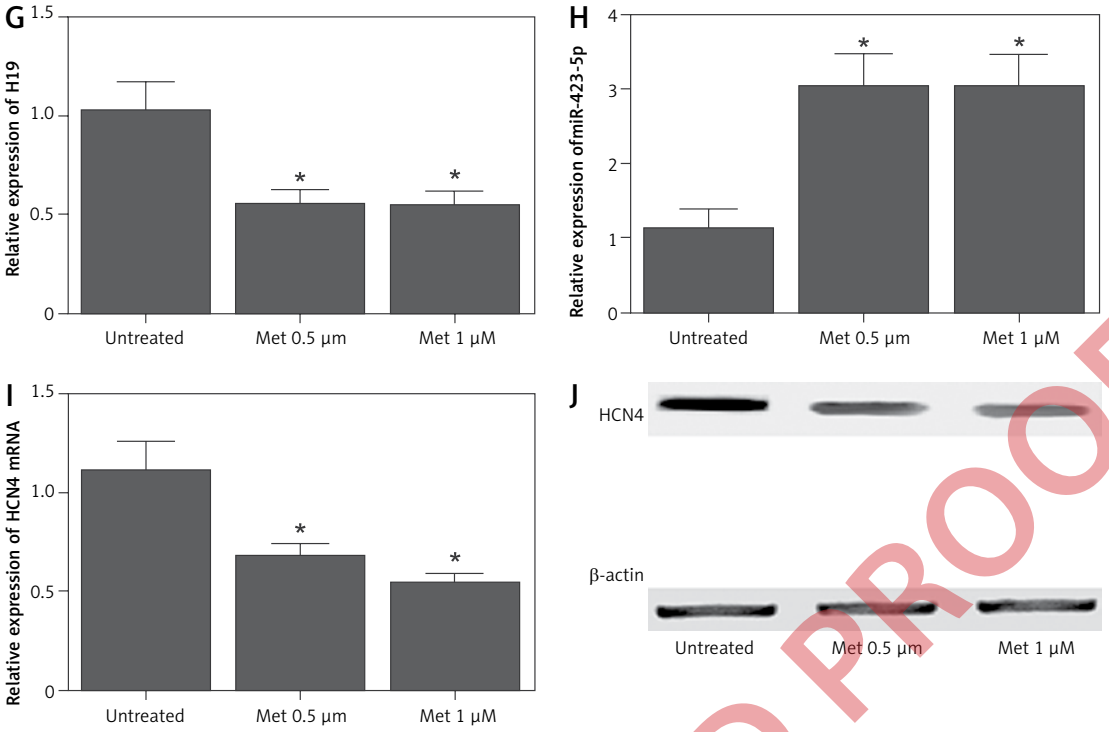

Figure 5. Cont. **G** – Level of H19 in H9C2 cells transfected with H19 siRNA 1 or H19 siRNA2 compared with that in H9C2 cells transfected with the negative control (*p-value < 0.05, vs. untreated cells). **H** – Level of miR-423-5p in H9C2 cells transfected with H19 siRNA 1 or H19 siRNA2 compared with that in H9C2 cells transfected with the negative control (*p-value < 0.05, vs. untreated cells). **I** – Level of HCN4 in H9C2 cells transfected with H19 siRNA 1 or H19 siRNA2 compared with that in H9C2 cells transfected with the negative control (*p-value < 0.05, vs. untreated cells). **J** – Western blot analysis of HCN4 protein expression in H9C2 cells transfected with H19 siRNA 1 or H19 siRNA2 compared with that in H9C2 cells transfected with the negative control (*p-value < 0.05, vs. untreated cells)

it has been shown that the presence of DM may reduce the therapeutic effect of IBD. Meanwhile, we found that MET may reduce the expression of H19 by enhancing the methylation status of its promoter, which subsequently increases the expression of miR-423-5p and suppresses the expression of its target, HCN4, an important player in the pathogenesis of CHF.

Conflicts of interest

The authors declare no conflict of interest.

References

1. McMurray JJ, Stewart S. Epidemiology, aetiology, and prognosis of heart failure. Heart 2000; 83: 596-602.
2. Mosterd A, Hoes AW. Clinical epidemiology of heart failure. Heart 2007; 93: 1137-46.
3. Maggioni AP, Dahlstrom U, Filippatos G, et al. EURObservational Research Programme: regional differences and 1-year follow-up results of the Heart Failure Pilot Survey (ESC-HF Pilot). Eur J Heart Fail 2013; 15: 808-17.
4. Ponikowski P, Voors AA, Anker SD, et al. 2016 ESC Guidelines for the diagnosis and treatment of acute and chronic heart failure: The Task Force for the diagnosis and treatment of acute and chronic heart failure of the European Society of Cardiology (ESC)Developed with the special contribution of the Heart Failure Association (HFA) of the ESC. Eur Heart J 2016; 37: 2129-2200.
5. Mozaffarian D, Benjamin EJ, Go AS, et al. Executive summary: Heart disease and stroke statistics – 2016 update: a report from the American Heart Association. Circulation 2016; 133: 447-54.
6. Biel M, Wahl-Schott C, Michalakis S, Zong X. Hyperpolarization-activated cation channels: from genes to function. Physiol Rev 2009; 89: 847-85.
7. Chu HY, Zhen X. Hyperpolarization-activated, cyclic nucleotide-gated (HCN) channels in the regulation of midbrain dopamine systems. Acta Pharmacol Sin 2010; 31: 1036-43.
8. Baruscotti M, Bottelli G, Milanesi R, DiFrancesco JC, DiFrancesco D. HCN-related channelopathies. Pflugers Arch 2010; 460: 405-15.
9. Biel M, Schneider A, Wahl C. Cardiac HCN channels: structure, function, and modulation. Trends Cardiovasc Med 2002; 12: 206-12.
10. Zwadlo C, Borlak J. Disease-associated changes in the expression of ion channels, ion receptors, ion exchangers and Ca(2+)-handling proteins in heart hypertrophy. Toxicol Appl Pharmacol 2005; 207: 244-56.
11. Zicha S, Fernandez-Velasco M, Lonardo G, L'Heureux N, Nattel S. Sinus node dysfunction and hyperpolarization-activated (HCN) channel subunit remodeling in a canine heart failure model. Cardiovasc Res 2005; 66: 472-81.
12. DiFrancesco D, Camm JA. Heart rate lowering by specific and selective I(f) current inhibition with ivabradine: a new therapeutic perspective in cardiovascular disease. Drugs 2004; 64: 1757-65.
13. Bois P, Bescond J, Renaudon B, Lenfant J. Mode of action of bradycardic agent, S 16257, on ionic currents of

rabbit sinoatrial node cells. Br J Pharmacol 1996; 118: 1051-7.
14. Yue-Chun L, Teng Z, Na-Dan Z, et al. Comparison of effects of ivabradine versus carvedilol in murine model with the Coxsackievirus B3-induced viral myocarditis. PLoS One 2012; 7: e39394.
15. Swedberg K, Komajda M, Bohm M, et al. Ivabradine and outcomes in chronic heart failure (SHIFT): a randomised placebo-controlled study. Lancet 2010; 376: 875-85.
16. Cao X, Sun Z, Zhang B, Li X, Xia H. The effects of ivabradine on cardiac function after myocardial infarction are weaker in diabetic rats. Cell Physiol Biochem 2016; 39: 2055-64.
17. Wu T, Qu L, He G, et al. Regulation of laryngeal squamous cell cancer progression by the lncRNA H19/miR-148a-3p/DNMT1 axis. Oncotarget 2016; 7: 11553-66.
18. Srivastava M, Hsieh S, Grinberg A, Williams-Simons L, Huang SP, Pfeifer K. H19 and Igf2 monoallelic expression is regulated in two distinct ways by a shared cis acting regulatory region upstream of H19. Genes Dev 2000; 14: 1186-95.
19. Kawakami T, Zhang C, Okada Y, Okamoto K. Erasure of methylation imprint at the promoter and ctcf-binding site upstream of h19 in human testicular germ cell tumors of adolescents indicate their fetal germ cell origin. Oncogene 2006; 25: 3225-36.
20. Yan L, Zhou J, Gao Y, et al. Regulation of tumor cell migration and invasion by the H19/let-7 axis is antagonized by metformin-induced DNA methylation. Oncogene 2015; 34: 3076-84.
21. Scarpello JH, Howlett HC. Metformin therapy and clinical uses. Diab Vasc Dis Res 2008; 5: 157-67.
22. Inzucchi SE, Bergenstal RM, Buse JB, et al. Management of hyperglycaemia in type 2 diabetes: a patient-centered approach. Position statement of the American Diabetes Association (ADA) and the European Association for the Study of Diabetes (EASD). Diabetologia 2012; 55: 1577-96.
23. Grzybowska M, Bober J, Olszewska M. Metformin – mechanisms of action and use for the treatment of type 2 diabetes mellitus. Postepy Hig Med Dosw (Online) 2011; 65: 277-85 [Article in Polish].
24. Sasaki H, Asanuma H, Fujita M, et al. Metformin prevents progression of heart failure in dogs: role of AMP-activated protein kinase. Circulation 2009; 119: 2568-77.
25. Xiao H, Ma X, Feng W, et al. Metformin attenuates cardiac fibrosis by inhibiting the TGFbeta1-Smad3 signalling pathway. Cardiovasc Res 2010; 87: 504-13.
26. Gundewar S, Calvert JW, Jha S, et al. Activation of AMP-activated protein kinase by metformin improves left ventricular function and survival in heart failure. Circ Res 2009; 104: 403-11.
27. Jin B, Ernst J, Tiedemann RL, et al. Linking DNA methyltransferases to epigenetic marks and nucleosome structure genome-wide in human tumor cells. Cell Rep 2012; 2: 1411-24.
28. Zhong T, Men Y, Lu L, et al. Metformin alters DNA methylation genome-wide via the H19/SAHH axis. Oncogene 2017; 36: 2345-54.
29. Noble D, Noble PJ. Late sodium current in the pathophysiology of cardiovascular disease: consequences of sodium-calcium overload. Heart 2006; 92 Suppl 4: iv1-iv5.
30. Hale SL, Kloner RA. Ranolazine treatment for myocardial infarction? Effects on the development of necrosis, left ventricular function and arrhythmias in experimental models. Cardiovasc Drugs Ther 2014; 28: 469-75.
31. Mourouzis I, Mantzouratou P, Galanopoulos G, et al. The beneficial effects of ranolazine on cardiac function after myocardial infarction are greater in diabetic than in nondiabetic rats. J Cardiovasc Pharmacol Ther 2014; 19: 457-69.
32. Sossalla S, Maier LS. Role of ranolazine in angina, heart failure, arrhythmias, and diabetes. Pharmacol Ther 2012; 133: 311-23.
33. Brede M, Wiesmann F, Jahns R, et al. Feedback inhibition of catecholamine release by two different alpha2-adrenoceptor subtypes prevents progression of heart failure. Circulation 2002; 106: 2491-6.
34. D'Souza A, Pearman CM, Wang Y, et al. Targeting miR-423-5p reverses exercise training-induced HCN4 channel remodeling and sinus bradycardia. Circ Res 2017; 121: 1058-68.
35. Oeing CU, Tschope C, Pieske B. The new ESC Guidelines for acute and chronic heart failure 2016. Herz 2016; 41: 655-63 [Article in German].
36. Sulfi S, Timmis AD. Ivabradine – the first selective sinus node I(f) channel inhibitor in the treatment of stable angina. Int J Clin Pract 2006; 60: 222-8.
37. Yusuf S, Camm AJ. Sinus tachyarrhythmias and the specific bradycardic agents: a marriage made in heaven? J Cardiovasc Pharmacol Ther 2003; 8: 89-105.
38. Fox K, Ford I, Steg PG, Tardif JC, Tendera M, Ferrari R. Ivabradine in stable coronary artery disease without clinical heart failure. N Engl J Med 2014; 371: 1091-9.
39. Leoni AL, Marionneau C, Demolombe S, et al. Chronic heart rate reduction remodels ion channel transcripts in the mouse sinoatrial node but not in the ventricle. Physiol Genomics 2005; 24: 4-12.
40. Suffredini S, Stillitano F, Comini L, et al. Long-term treatment with ivabradine in post-myocardial infarcted rats counteracts f-channel overexpression. Br J Pharmacol 2012; 165: 1457-66.
41. Chiha M, Njeim M, Chedrawy EG. Diabetes and coronary heart disease: a risk factor for the global epidemic. Int J Hypertens 2012; 2012: 697240.
42. Donahoe SM, Stewart GC, McCabe CH, et al. Diabetes and mortality following acute coronary syndromes. JAMA 2007; 298: 765-75.
43. Carrabba N, Valenti R, Parodi G, Santoro GM, Antoniucci D. Left ventricular remodeling and heart failure in diabetic patients treated with primary angioplasty for acute myocardial infarction. Circulation 2004; 110: 1974-9.
44. Shi YQ, Yan M, Liu LR, et al. High glucose represses hERG K+ channel expression through trafficking inhibition. Cell Physiol Biochem 2015; 37: 284-96.
45. Davis D, Sinoway LI, Robison J, et al. Norepinephrine kinetics during orthostatic stress in congestive heart failure. Circ Res 1987; 61 (4 Pt 2): I87-90.